UDC 541.135.3 : 669.295
DOI dx.doi.org/10.17073/1997-308X-2022-4-14

Electrode processes in the production of microdispersed titanium powder by volumetric electrolytic reduction of its ions with sodium dissolved in the $BaCl_2$—$CaCl_2$—NaCl melt in the absence of titanium halides in the initial melt

© 2022 г. **V.A. Lebedev, V.V. Polyakov**

Ural Federal University n.a. the first President of Russia B.N. Eltsin, Ekaterinburg, Russia

Received 01.03.2022, revised 17.06.2022, accepted for publication 21.06.2022

Abstract: The paper is devoted to a detailed study of cathodic processes, their influence on the anode process, and electrolysis performance. The polarization of a steel cathode in a $CaCl_2$—$BaCl_2$—NaCl melt at t = 610 °C was measured. The polarization curve clearly shows the potentials and current densities of the formation of a saturated sodium solution in the electrolyte (E_{sat} = —2.97 V, i_c = 0.04 A/cm^2, lgi_c = —1,4), and the occurrence of sodium metal on the cathode (E_{Na} = —3.22 V, i_{Na} = 0.12 A/cm^2, lgi_{Na} = —0.92). The value of E_{sat} was used to calculate the concentration of sodium in the electrolyte at t = 610 °C ($1.3 \cdot 10^{-4}$ mol. fr.). The values of E_{sat}, E_{Na}, and their difference (ΔE = 0,25 B) were confirmed by long-term electrolysis. These fundamental characteristics are the basis for process control and management. During long-term electrolysis, on the curve in the coordinates E (V) — lg$Q$ (A·min), 3 regions close to rectilinear ones were revealed: the discharge of sodium ions from supersaturated solutions at E more negative than E_{sat} (from E_{Na} to E_{sat}), from mixtures of supersaturated and saturated solutions (at a constant E equal to E_{sat}), from diluted solutions (with E more positive than E_{sat}). The activity coefficients of sodium in supersaturated solutions are close to 1, which ensures their increased reducing ability. Maximum degrees of supersaturation (>100) are created at formation and decomposition on the cathode of metallic sodium nuclei, which are sufficient to intensify and prolong electrolysis, to lower the lower temperature limit of its realization from 600 to 350 °C. The formation of metallic titanium in the near-anode layer is explained by the disproportionation of Ti^{2+} ions entering the near-anode electrolyte from the anode surface and from the near-cathode melt.

Keywords: electrolytic bulk reduction of titanium, additive technologies, granulometry, potentials and current densities of formation of saturated solutions and metallic sodium on the cathode, nucleation and decay parameters of sodium nuclei, required degrees of supersaturation for their appearance on the cathode.

Lebedev V.A. — Dr. Sci. (Chem.), prof., Department of metallurgy of non-ferrous metals of Ural Federal University n.a. the first President of Russia B.N. Eltsin (UrFU) (620002, Russia, Sverdlovsk region, Ekaterinburg, Mira str., 19).
E-mail: v.a.lebedev@urfu.ru.

Polyakov V.V. — educational master, postgraduate student, Department of metallurgy of non-ferrous metals, UrFU.
E-mail: aheon@mail.ru.

For citation: *Lebedev V.A., Polyakov V.V.* Electrode processes in the production of microdispersed titanium powder by volumetric electrolytic reduction of its ions with sodium dissolved in the $BaCl_2$—$CaCl_2$—NaCl melt in the absence of titanium halides in the initial melt. *Izvestiya Vuzov. Poroshkovaya Metallurgiya i Funktsional'nye Pokrytiya (Powder Metallurgy and Functional Coatings)*. 2022. Vol. 16. No. 4. P. 4—14 (In Russ.). DOI: dx.doi.org/10.17073/1997-308X-2022-4-14.

Электродные процессы при получении микродисперсного порошка титана объемным электролитическим восстановлением его ионов натрием, растворенным в расплаве $BaCl_2$—$CaCl_2$—NaCl, в отсутствие галогенидов титана в исходном расплаве

В.А. Лебедев, В.В. Поляков

Уральский федеральный университет (УрФУ) им. первого Президента России Б.Н. Ельцина, г. Екатеринбург, Россия

Статья поступила в редакцию 01.03.2022 г., доработана 17.06.2022 г., подписана в печать 21.06.2022 г.

Аннотация: Работа посвящена детальному изучению катодных процессов, их влиянию на анодный процесс и показатели электролиза. Измерена поляризация стального катода в расплаве $CaCl_2$—$BaCl_2$—NaCl при температуре t = 610 °C. На по-

ляризационной кривой отчетливо выделяются потенциалы ($E_{нас}$ = —2,97 В) и плотности тока ($i_к$ = 0,04 А/см^2, lg$i_к$ = —1,4) образования насыщенного раствора натрия в электролите и появления металлического натрия на катоде (E_{Na} = —3,22 В, i_{Na} = 0,12 А/см^2, lgi_{Na} = —0,92). По величине $E_{нас}$ рассчитана концентрация натрия в электролите при t = 610 °С ($1{,}3\cdot10^{-4}$ мол. дол.). Величины $E_{нас}$, E_{Na} и их разность (ΔE = 0,25 В) подтверждены при длительном электролизе. Эти фундаментальные характеристики являются основой для контроля и управления процессом. При длительном электролизе на кривой в координатах E (В) — lg$Q$ (А·мин) выявлены 3 близких к прямолинейным участка: разряд ионов натрия из пересыщенных растворов при E отрицательнее $E_{нас}$ (от E_{Na} до $E_{нас}$), из смеси пересыщенных и насыщенных растворов (при постоянном E, равным $E_{нас}$), из разбавленных растворов (при E положительнее $E_{нас}$). Коэффициенты активности натрия в пересыщенных растворах близки к 1, что обеспечивает их повышенную восстановительную способность. Максимальные степени пересыщения (>100) создаются при образовании и распаде на катоде зародышей металлического натрия, которые достаточны для того, чтобы интенсифицировать и продлить электролиз, понизить нижний предел температур его реализации с 600 до 350 °С. Образование металлического титана в прианодном слое объяснено диспропорционированием ионов Ti^{2+}, поступающих в прианодный электролит от поверхности анода и из прикатодного расплава.

Ключевые слова: электролитическое объемное восстановление титана, аддитивные технологии, гранулометрия, потенциалы и плотности тока образования на катоде насыщенных растворов и металлического натрия, параметры зарождения и распада зародышей натрия, необходимые степени пересыщения для их появления на катоде.

Лебедев В.А. — докт. хим. наук, проф. кафедры металлургии цветных металлов УрФУ (620002, Свердловская обл., г. Екатеринбург, ул. Мира, 19). E-mail: v.a.lebedev@urfu.ru.

Поляков В.В. — учебный мастер, аспирант кафедры металлургии цветных металлов УрФУ. E-mail: aheon@mail.ru.

Для цитирования: *Лебедев В.А., Поляков В.В.* Электродные процессы при получении микродисперсного порошка титана объемным электролитическим восстановлением его ионов натрием, растворенным в расплаве $BaCl_2$—$CaCl_2$—NaCl, в отсутствие галогенидов титана в исходном расплаве. *Известия вузов. Порошковая металлургия и функциональные покрытия*. 2022. Т. 16. No. 4. С. 4—14. DOI: dx.doi.org/10.17073/1997-308X-2022-4-14.

Introduction

The constant growth in the production and use of titanium alloys is due to their unique properties — such as corrosion resistance, low specific gravity, mechanical strength at high temperatures, and biocompatibility. Titanium-based alloys are widely used in aircraft and space construction, rocket and missile engineering, automotive engineering, shipbuilding, medicine [1—3], and the chemical industry.

The theoretical foundations of the process of volumetric electrolytic preparation of microstructural metal powders for modern technology have been developed under the guidance of Prof. M.V. Smirnov [4], who demonstrated high reactivity [5] and mobility [6] of this process.

The purpose of this work was to provide scientific justification for the possibility of implementing the process of volumetric intensive electrochemical method developed by the authors for obtaining microdispersed titanium powders for 3D technologies and powder metallurgy [7, 8]. The uniqueness of the process lies in the fact that it is carried out in the absence of dissolved sodium and titanium chlorides in the initial and final electrolytes (unlike the work [9]), with a stepwise increase in the electrolysis current and potentiometric control of the process [10].

To solve this problem, an original method for monitoring and controlling the process under development by measuring the RedOx-potential of the Ti^{3+}/Ti^{2+} system in the near-anode layer was proposed and applied in practice. As a result, the mechanisms of the process realization at the initial, main and final stages of electrolysis are disclosed.

It is shown that in the first 12 min of electrolysis, the concentration of inactive Ti^{3+} complex ions increases in the near-anode layer, and sodium dissolved in the electrolyte restores mainly Ti^{2+} ions in the electrolyte volume. Starting from the 20^{th} minute of electrolysis, as titanium powder accumulates in the electrolyte bulk, the concentration of Ti^{2+} ions begins to increase rapidly in the near-anode layer according to the reaction $2Ti^{3+} + Ti = 3Ti^{2+}$. At the same time, the proportion of sodium consumed for the reduction of Ti^{3+} to Ti^{2+} decreases. This contributes to an increase in the current output and stabilization of the cathode potential for 30 min at E_c = —2.96 V. After 50 min of electrolysis, the reactivity of the salt melt begins to decrease due to the low solubility of sodium in it. The cathode potential decreases sharply towards positive values. The concentration of Ti^{3+} ions in the near-anode layer increases steadily until it aligns at 85 min with the

concentration of Ti^{2+} ions. This dramatically increases the current consumption for ion recharge and leads to the need to stop electrolysis after a short-term (for 40 s) switching on the current of 12 A. After 10 s, judging by the change in the cathode potential, almost all of the sodium dissolved in the electrolyte is consumed for the reduction of titanium ions. After 6 min, the potentials of the electrodes returned to the initial value of the anode potential, indicating a return of the system to its initial state, where titanium salts and dissolved sodium were absent. More than 95 % of the powder is obtained in the volume of the electrolyte. The current yield was 84.0 % and was close to the calculated average valence of titanium ions in the near-anode layer and mass loss of the anode (87.0 %).

This paper is devoted to a detailed analysis of the mechanism of the cathode process, its effect on the anode process, and the results of electrolysis.

The methodology of the experiment

The experiments were carried out at t = 610 °C in a eutectic composition melt, mol. fr.: $BaCl_2$ — 0.16; $CaCl_2$ — 0.47; NaCl — 0.37, with t_{melt} = 452 ± 2 °C. Low-melting electrolytes similar in composition are used in industry to produce sodium with high current efficiency. The electrolyte was prepared from predehydrated salts according to the method [11]. Titanium salts and metallic sodium were not added to the original electrolyte.

The design of the electrolytic cell is shown in Fig. 1.

Prior to the experiment, 228 g of electrolyte was loaded into the crucible. The anode is made of a titanium rod (current conductor) weighing 23.36 g and a titanium plate weighing 14.18 g. The walls of a steel crucible were used as the cathode. The working surface area of the anode was 14.4 cm^2, the cathode was 100 cm^2. To completely dry the electrolyte, the cell was heated under vacuum to 400° C, then argon purified by passing it through a titanium chip heated to 820 °C was supplied.

Polarization studies were carried out on the chassis of the NI PXIe 8108 instrument (National Instruments, USA) with NI PXI-4140, NI PXI-4072, and NI PXIe-6356 modules. The application for this device is written in the graphical programming language LabVIEW 10. The duration of the current pulse was 10 s, then the current was switched off for 10 s with measurement of the electrode potential value 0.5 ms after switching off, then the next current value was switched on for 10 s. The sequential increase in current was uniform on a logarithmic scale: 1.0, 1.59, 2.51, 3.98, 6.31, 10.0 in each period.

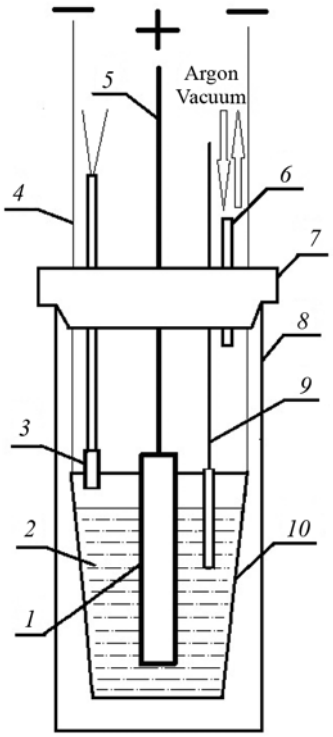

Fig. 1. Design of an electrolytic cell

1 — titanium plate (VT1-0); ***2*** — electrolyte; ***3*** — chromel-alumel thermocouple in BeO sheath; ***4*** — crucible steel suspension (cathode); ***5*** — titanium rod (current conductor); ***6*** — branch pipe for evacuating air and supplying argon; ***7*** — vacuum rubber stopper; ***8*** — quartz cell; ***9*** — reference electrode in BeO sheath; ***10*** — steel crucible

Рис. 1. Устройство электролитической ячейки

1 — титановая пластина (ВТ1-0); ***2*** — электролит; ***3*** — хромель-алюмелевая термопара в чехле из BeO; ***4*** — стальной подвес тигля (катод); ***5*** — титановый стержень (токоподвод); ***6*** — патрубок для откачки воздуха и подачи аргона; ***7*** — пробка из вакуумной резины; ***8*** — кварцевая ячейка; ***9*** — электрод сравнения в чехле из BeO; ***10*** — стальной тигель

A lead electrode KCl—NaCl + 10 wt.% $PbCl_2$ was used as a reference electrode.

$$E\,[\text{V}] = -1.79 + 0.42\cdot10^{-3}T, \quad E_{883\,\text{K}} = -1{,}42\ \text{V}. \quad (1)$$

The results were recalculated on a chlorine electrode.

Results and discussion

The results of the cathode polarization study are shown in Fig. 2 in E_c—lgi_c coordinates.

At the current of I_c = 4 A (cathodic current density i_c = 0.04 A/cm^2, lg0.04 = –0.92) is obtained by sodium saturation of cathode electrolyte at E_{sat} = –2.97 V.

At I_c = 12 A (i_c = 0.12 A/cm^2, lg0.12 = –1.4) the cathode potential –3.22 V is close to the conditional standard sodium deposition potential –3.32 V, but doesn't reach it by 0.10 V. The sodium deposition potential (E^*) was calculated according to the procedure [12], using the values of standard potential of the Na^+/Na system in NaCl [4]:

$$E^0 = -3.903 + 0.60\cdot10^{-3}T, \quad E^0_{883\ K} = -3.373\ V, \tag{2}$$

as well as mole fractions and ionic moments of cations, nm^{-1}: Na^+ — 10.2, Ca^{2+} — 19.23, and Ba^{2+} — 14.5 in the electrolyte used:

$$E^* = -3.829 + 0.58\cdot10^{-3}T, \quad E^*_{883\ K} = -3.32\ V, \tag{3}$$

$$E^* - E^0 = 0.074 - 0.02\cdot10^{-3}T, \quad \Delta E_{883\ K} = 0.0563\ V. \tag{4}$$

By dividing the values given in equation (4) by the value of the pre-logarithmic coefficient ($2.3RT/F$ = $= 2.3\cdot8.314\cdot883/96485 = 0.175$, where R is the universal gas constant, F is the Faraday constant; T is temperature, K), the equation was obtained for calculating the value of activity coefficient of sodium ions in a salt melt (γ) and its value at T = 883 K:

$$\lg\gamma = 0.423 - 0.114\cdot10^{-3}T, \quad \lg\gamma = 0.322, \quad \gamma_{883\ K} = 2.1. \tag{5}$$

The sodium activity in the melt used ($0.37\cdot2.1 = 0.78$) is close to 1, hence the activity of supercooled NaCl.

Information about the sequence and trends of electrode processes is obtained by measuring the changes in electrode potentials over time after the electrolysis current is switched off.

For the cathodic process (Fig. 3) at I = 2, 4, and 6 A, relatively stable (within 20 s) values of the cathode potentials are observed. At the same time, two processes occur on them: the decline in concentration polarization, which shifts the potential of the cathode toward positive values, and the influx of sodium dissolved in the salt from the electrolyte volume to the cathode surface, which shifts its potential in the opposite direction. For the first and second periods of electrolysis with a current of 2 A, the first process prevails.

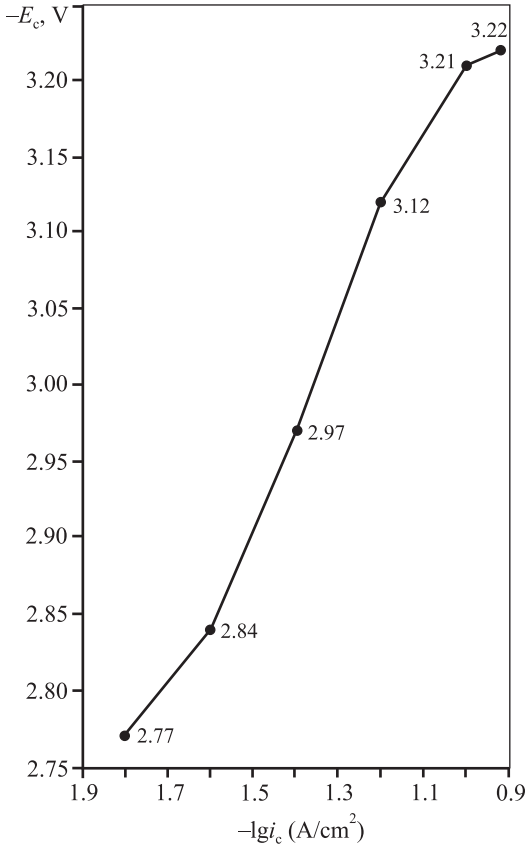

Fig. 2. Results of the cathode polarization study

Рис. 2. Результаты изучения поляризации катода

After electrolysis with 4 and 6 A currents, the process rates equalize, and the cathode potential stabilizes at –2.97 V. With the same value, the cathode potential begins to shift towards positive values after the current is turned off 8 A.

Studies carried out by different methods suggest that the cathode potential of –2.97 ± 0.01 V is a fundamental characteristic corresponding to a saturated sodium solution in the electrolyte used at t = 610 °C (E_{sat}). The sodium activity in a saturated solution (asat) was calculated based on the assumption that a change in the cathode potential from –3.22 to –2.97 V (i.e., by 0.25 V) is associated with a change in the activity of dissolved sodium. By substituting the corresponding values for the electrolyte used, we obtain $\lg a_{sat} = -0.25/0.175 = -1.486$, $a_{sat} = 0.0373$. Dividing this value by the activity coefficient of sodium (288), we obtain the sodium concentration in a saturated solution ($1.3\cdot10^{-4}$ mol. fr.).

Starting from I = 8 A, a sharper shift of the cathode potentials towards positive values is observed (see Fig. 3), which increases at I = 10 A. After the first switching off of 10 A current (see Fig. 5, per. *6*), the potential

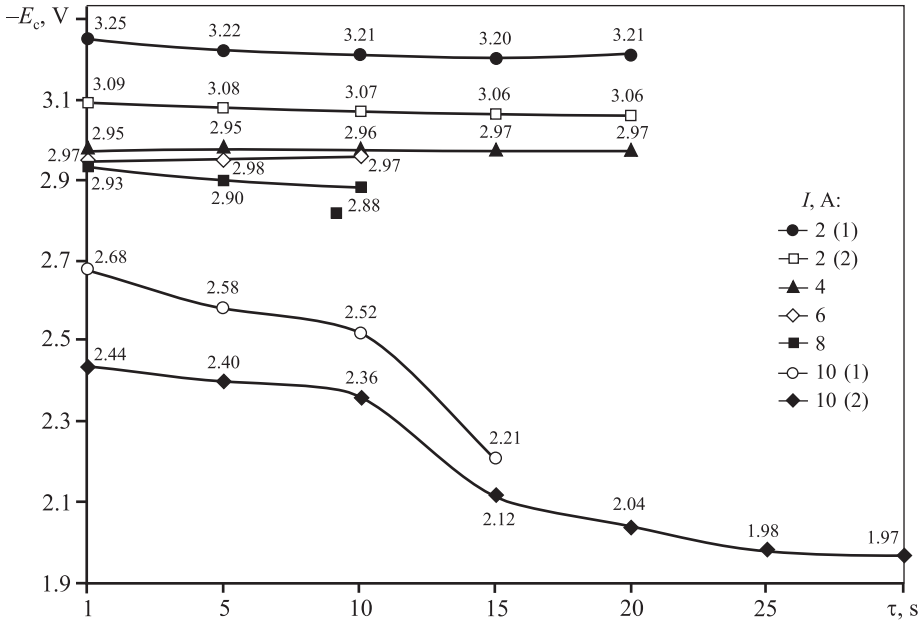

Fig. 3. Change in time of the cathode potential after the electrolysis current is switched off

Рис. 3. Изменение во времени потенциала катода после отключения тока электролиза

of –2.68 V corresponded to the concentration of dissolved sodium of $5 \cdot 10^{-3}$ mol. fr., which was enough to reduce the concentration of Ti^{2+} ions after 5 s down to $2.5 \cdot 10^{-7}$ mol. fr. (E_c = –2.58 V), and after 10 s — down to $6 \cdot 10^{-6}$ mol. fr. (E_c = –2.52 V). After the second switching off of 10 A current, the sodium concentration decreases down to $1 \cdot 10^{-5}$ mol. fr. (E_c = –2.44 V). After 5 s the concentration of Ti^{2+} ions was reduced down to $2 \cdot 10^{-5}$ mol. fr. (E_c = –2.48 V), after 10 s — down to $1 \cdot 10^{-5}$ mol. fr. (E_c = –2.36 V). With a further decrease in the cathode potential, the system under consideration passes into the area of coexistence of Ti^{2+} and Ti^{3+} ions. The ratio of Ti^{2+}/Ti^{3+} ion concentrations equal to 100 corresponds to the steady-state potential of –1.97 V. The appearance of the curves of the cathode potential change with time, observed when the current of 10 A is switched off, is similar at lower electrolysis currents as well. It is always necessary to wait for the transition of the system to the region of coexistence of Ti^{2+} and Ti^{3+} ions to exclude the presence of an alkali metal and noticeable amounts of titanium ions in the final electrolyte.

The time variation of the anode potentials after switching off the electrolysis current is shown in Fig. 4.

When currents 2, 4, and 6 A are switched off, the anode potentials naturally shift toward negative values under the influence of the richer Ti^{2+} ions of the melt in the pre-cathode space. For I = 8 A, the RedOx potential does not exceed —1.75 V, which corresponds to 5-fold excess of the Ti^{2+} ion proportion. When switching off the current of 10 A, briefly, in 5—10 s, the maximum potential values are reached (–1.835 V, –1.831 V), corresponding to the ratio of ions Ti^{2+}/Ti^{3+} = 20÷17. After τ = 5 s, they decrease to —1.8 V, the ratio of ions Ti^{2+}/Ti^{3+} = 10. The presence of two fluxes of Ti^{2+} ions from the cathode side and the anode surface leads not to the expected increase, but to a rapid decrease in the concentration of Ti^{2+} ions due to the implementation of the disproportionation reaction:

$$3Ti^{2+} = 2Ti^{3+} + Ti. \quad (6)$$

We associate the formation of finely dispersed grains of metallic titanium in the form of linear and bulk aggregates in the near-anode electrolyte with the development of this reaction. This is due to the reaction taking place at a distance from the anode that is less than the thickness of the diffusion layer [13, 14].

Prolonged electrolysis was carried out with a step-by-step increase in current. Fig. 5 shows the operating voltage, cathode and anode potentials, inverse EMF, current values and duration of electrolysis in each of the 7 periods. All measurements were performed with an accuracy of 1 mV. This made it possible to trace the change in the ratio of Ti^{3+} and Ti^{2+} titanium ions in the near-anode layer and the change in the RedOx potential in the near-cathode layer of the electrolyte.

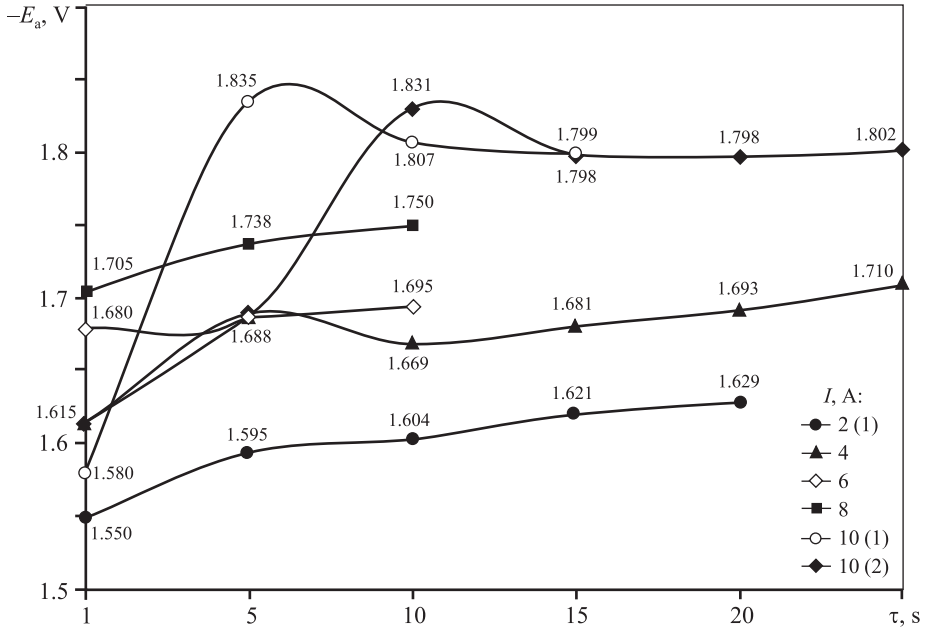

Fig. 4. Change of the anode potential in time after the electrolysis current is switched off

Рис. 4. Изменение потенциала анода во времени после отключения тока электролиза

Conditional standard potentials of systems Ti^{3+}/Ti, Ti^{2+}/Ti, Ti^{3+}/Ti^{2+} for $CaCl_2$, $BaCl_2$, NaCl were taken from the monograph [4]. By multiplying the corresponding values by the mole fractions of the components and adding the results obtained, we obtained equations to calculate the conditional standard potentials of the corresponding systems in the electrolyte used. The coefficients of the equations $E^* = A + 10^{-3}BT$ are given in Table 1.

Based on the initial (before electrolysis) potentials of the cathode (–2.48 V) and anode (–1.87 V), the concentrations of the corresponding ions in the electrode layers were calculated. For the cathode they are equal to, mol. fr.: Ti^{2+} — $5.2\cdot10^{-7}$, Ti^{3+} — $4.8\cdot10^{-12}$. Ti^{3+}/Ti^{2+} concentration ratio makes up ~$1\cdot10^{-5}$. For the anode this ratio equals to $3.7\cdot10^{-2}$, and average valency is 2.04.

The given values of conditional standard potentials made it possible to describe the processes occurring at the electrodes during electrolysis.

The reactivity of sodium dissolved in the electrolyte naturally decreases with an increase in the electricity

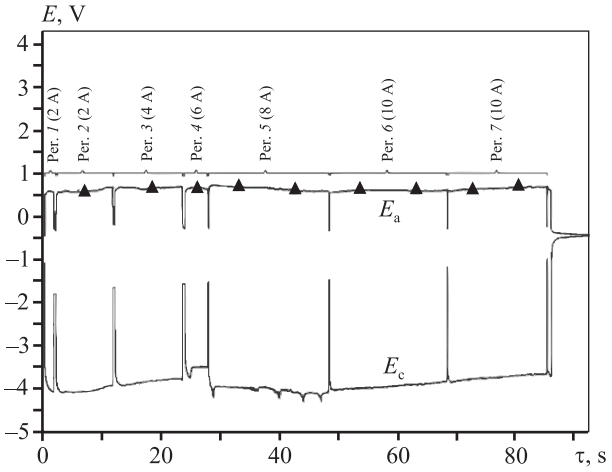

Fig. 5. Scheme of implementation of long-term electrolysis

Рис. 5. Схема реализации длительного электролиза

Table 1. **Results of calculating the values of conditional standard potentials of the systems Ti^{2+}/Ti, Ti^{3+}/Ti, Ti^{3+}/Ti^{2+} in the electrolyte used**

Таблица 1. Результаты расчета величин условных стандартных потенциалов систем Ti^{2+}/Ti, Ti^{3+}/Ti, Ti^{3+}/Ti^{2+} в используемом электролите

Salt	$E^*_{Ti^{2+}/Ti}$, V		$E^*_{Ti^{3+}/Ti}$, V		$E^*_{Ti^{3+}/Ti^{2+}}$, V	
	$-A$	B	$-A$	B	$-A$	B
$CaCl_2$	2.48	0.68	2.24	0.55	1.78	0.29
$BaCl_2$	2.60	0.73	2.36	0.59	1.87	0.31
NaCl	2.42	0.51	2.19	0.34	1.74	0.01
Electrolyte	2.49	0.63	2.24	0.48	1.78	0.18
$E^*_{883\ K}$, V	–1.93		–1.82		–1.62	

passed, and hence the amount of titanium powder accumulating in the salt melt (Fig. 6).

It is no coincidence that the duration of our experiments and the authors of the work [15] was approximately the same and was ~2 h, which is due to the need to limit the accumulation of titanium powder in the electrolyte. The authors of [15] noted that when 8—10 % of titanium is accumulated in the electrolyte, an increase in current does not result in an increase in the amount of metal produced, and at 20 % Ti, a drop in the operating voltage down to 0 was detected when the anode was short-circuited to the bottom of the crucible. This may be due to the appearance of noticeable electronic conductivity in such melts.

On the dependence of the cathode potential on the logarithm of the electricity transmitted (see Fig. 6) there are three close to rectilinear regions.

The straight line equation in the region from –3.225 to –2.951 V is

$$E\,[\mathrm{V}] = -3.32 + 0.185\lg Q \pm 0.011. \qquad (7)$$

The value of —3.32 coincides with the value of the conditional standard potential of sodium in the electrolyte used (3). The value of the prelogarithmic coefficient of 0.185 is close to its value for a single-electron process (2.3·8.314·883/96484 = 0.175), which indicates the constancy and proximity to 1 of the sodium activity coefficient in supersaturated solutions. The existence of the above region on the polarization curve was mentioned by the authors of [5] without explaining what processes it is associated with. In our opinion, it can be the formation (when current is flowing) and decay (when it is turned off for 10 s) of supersaturated solutions, the appearance and growth of electronic conductivity with the accumulation of powdered titanium in the salt melt. The deviation of the prelogarithmic coefficient from 0.175 may be considered as the occurrence and accumulation in the electrolyte of ions with a valency less than 1, for example, Na^{2+}. The first version seems to us the most probable on the considered part of the curve E—lg$Q$.

In our opinion, the long-term region of potential constancy at $E_c = -2.97 \pm 0.01$ V is associated with the coexistence of saturated and supersaturated sodium solutions in the electrolyte in the near-cathode layer. The decomposition of the latter makes it possible to stabilize the cathode potential. At potentials negative to –2.97 V, only supersaturated solutions exist. At a potential of –2.951 V, a saturated solution appears, the proportion of which increases as the amount of electricity passes further. At lg$Q$ = 2.41 (E_c = –2.962 V) which is

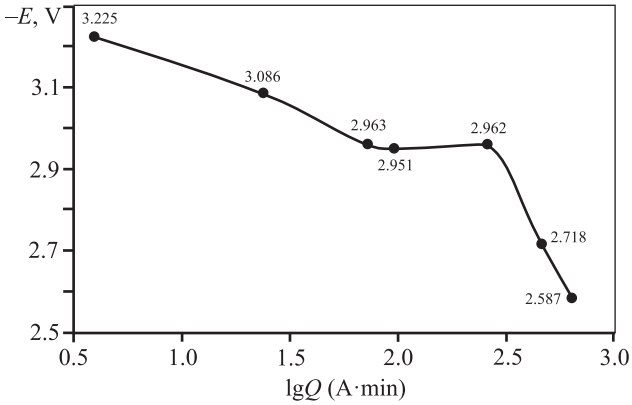

Fig. 6. The dependence of the cathode potential when the electrolysis current is switched off on the amount of electricity passed

Рис. 6. Зависимость потенциала катода при отключении тока электролиза от количества пропущенного электричества

in good agreement with the previously given value of 2.97 ± 0.01 V, all the supersaturated solution is consumed. The reactivity of sodium decreases hundreds of times, which is manifested in a sharp shift in the cathode potential towards positive values.

It should be noted that the characteristic points: E_{sat} = –2.97 V (formation of saturated solutions) and E_{Na} = –3.22 V (occurrence of a metallic sodium phase), were clearly manifested in the study of cathodic polarization with increasing electrolysis current and long-term electrolysis when the reducing ability of the melt decreased with an increase in the amount of electricity passed, and hence the amount of titanium powder accumulated in the electrolyte.

The most effective way to intensify and prolong electrolysis is the nucleation and decomposition of the metallic sodium phase at the cathode. It was observed at I = 6 and 8 A (see Fig. 5). An enlarged fragment of Fig. 5 is shown in Fig. 7. We associate the pulsating nature of the cathode potential change with the polarization accompanying the nucleation and decay of the liquid metallic sodium phase on the surface of the steel cathode.

When a current of 6 A is turned on (i_c = 0.06 A/cm^2 for the entire cathode surface bordering the melt), a voltage spike of 0.25 V, typical for phase polarization, is observed. The time to reach the maximum is 34 s, the decomposition time is 16 s, and the lifetime of the nucleus is 50 s. These parameters differ significantly from the respective values during the deposition of solid phases on a solid cathode, where the value of the maximum overvoltage varies from 20—30 to 70—100 mV, and the

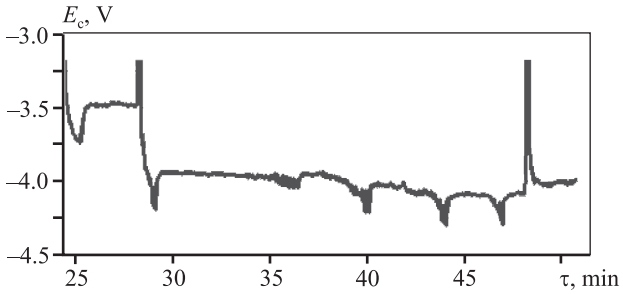

Fig. 7. Enlarged fragment of Fig. 5

Рис. 7. Увеличенный фрагмент рисунка 5

time to reach it varies from 10^{-2} до 10^{-4} s with a change in current density from 10^{-3} to 10^{-1} A·cm^2 [16]. The peculiarity of these curves is the slow reaching of the maximum and the rapid decay. After the decay of the nucleus in question, the cathode potential remained stable over time, and the difference between it and the maximum value remained 0.25 V.

When a current of 8 A (i_c = 0.08 A/cm^2) was turned on, the magnitude of the maximum overvoltage (0.25 V) was maintained, the nucleus lifetime was 36 s, the time to reach the maximum overvoltage was 27 s, and the decay time was 9 s. The rapid and accelerating decay is due to the high mobility of the resulting decay products, which spread throughout the volume of the electrolyte. After the decay of this nucleus, the cathode potential began to shift toward negative values at a rate of 0.10—0.15 mV/s due to the entry of dissolved sodium into the interelectrode space from the electrolyte volume. The increasing supersaturation of the cathode melt should have contributed to the formation of the following nuclei. Indeed, after 7 min, there was an attempt to nucleate the next nucleus, but it failed due to insufficient reactivity of the melt and a low degree of supersaturation in the pre-cathode space. For the occurrence of the next nucleus, the supersaturation of the melt increased up to 35 mV (the degree of supersaturation — 1.6), for the third one — 70 mV (the degree of supersaturation — 2.5), for the fourth one — 120 mV (the degree of supersaturation — 5.0). The maximum degree of saturation is observed during the formation and decay of sodium metal nuclei. In this case, the degree of supersaturation increases by more than 20 times ($10^{0.25/0.175} \approx 27$).

As a result of going through the stages of disintegration of supersaturated solutions, nucleation, and decay of metallic sodium nuclei in the volume of electrolyte the concentration of dissolved sodium was accumulated, which was enough to conduct electrolysis with 10 A current for 35 min and return the electrolyte composition to its original state.

In paper [5], the values of the solubility of Na in NaCl are given: at t = 816 °C — 2.42 mol.%, at t = = 864 °C — 4.06 mol.%. Based on these data, the temperature dependence of the Na solubility (N, mol. fr.) and the value of N at T = 1173 K and for a supercooled melt at T = 883 K were calculated:

$$\lg N = 3.817 - (5920/T),$$
$$N_{1173\ K} = 0.059, \quad N_{883\ K} = 0.0013. \tag{8}$$

In the same paper, an equation was given for calcu-

Table 2. **The results of calculating the sodium activity in the NaCl melt and the required degree of supersaturation to obtain metallic sodium on the cathode**

Таблица 2. Результаты расчета активности натрия в расплаве NaCl и необходимой степени пересыщения для получения на катоде металлического натрия

T, K	N, mol. fr.	lg$N$	lgγ	γ	lg$a$	a	Required degree of supersaturation
1173	0.059	–1.23	1.194	15.6	–0.04	0.92	1.09
1073	0.020	–1.700	1.879	75.7	–0.029	0.935	1.51
973	0.0055	–2.267	2.196	143	—0.123	0.79	1.27
873	0.0011	–2.962	2.498	315	–0.464	0.343	2.9
823	0.00042	–3.376	2.700	501	–0.68	0.211	4.8
773	0.00014	–3.841	2.927	845	–0.924	0.127	8.2
723	0.000043	–4.371	3.187	1540	–1.184	0.065	15
673	0.0000105	–4.979	3.486	3060	–1.49	0.032	31
623	0.0000021	–5.685	3.830	6761	–1.854	0.014	71

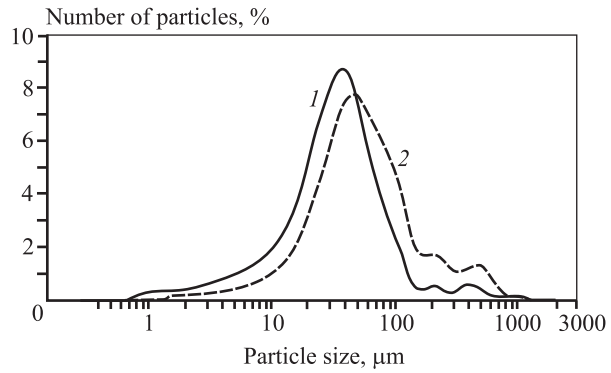

Fig. 8. Particle size distribution analysis of titanium powder

1 — after ultrasonic grinding; ***2*** — before ultrasonic grinding

Рис. 8. Гранулометрический анализ титанового порошка

1 — после ультразвукового измельчения

2 — до ультразвукового измельчения

lating the activity factor of sodium (γ) dissolved in the Na—NaCl melt:

$$\lg\gamma = (-0.823 + 2899/T)/(1 + 6.06(N_{Na}/(1 - N_{Na})). \quad (9)$$

Maximum values of Na in NaCl activity factors (γ) are calculated at $N_{Na} = 0$, $\gamma = 44.5$ ($T = 1173$ K) and 288 ($T = 883$ K).

Table 2 summarizes the results of calculating the activity of sodium (*a*) in the NaCl melt depending on the temperature and concentration of dissolved sodium (*N*).

At temperatures above 973 K, the required degrees of supersaturation are negligible; below 873 K they increase markedly, but even at $T = 623$ K (71) they are inferior to the maximum degrees of supersaturation during the formation and decay of metallic sodium nuclei (100—123 times). This makes it possible to lower the lower temperature limit of the process implementation from 600 to 350 °C.

According to the granulometric analysis (Fig. 8) (Institute of Thermal Energy of Ural Branch of RAS, Ekaterinburg), 95 % of the obtained titanium powder is in the melt volume in the form of aggregates, easily crushed into individual crystals. More than 80 % of these crystals are in the range of 10—100 μm with an average size of 36 μm, which meets the requirements for the size of powders for additive technologies.

Conclusion

A preliminary study of the cathode polarization revealed the potentials and current densities of sodium saturation of the salt melt ($E_{sat} = -2.97$ V, $i = 0.04$ A/cm^2) and the occurrence of sodium metal on the cathode ($E_{Na} = -3.22$ V, $i_c = 0.12$ A/cm^2). The concentration of sodium in a saturated solution at $t = 610$ °C ($1.3 \cdot 10^{-4}$ mol. fr.) was calculated using the value of E_{sat}. The values of E_{sat}, E_{Na}, and the difference between them ($\Delta E = 0.25$ V) have been confirmed in long-term electrolysis and are the basis for monitoring and controlling the process.

During prolonged electrolysis, three regions close to rectilinear were identified on the curve in coordinates E (B) — lg$Q$ (A·min). In the equation of the straight line $E = A + B\lg Q$ in the region from –3.22 to –2.963 V, the value of A (–3.32 V) coincides with the value of the conditional standard potential of sodium in the electrolyte used. The value of B (0.185 V) is close to its value for the one-electron process (0.175), which indicates the constancy and closeness to 1 of the activity coefficient of sodium in supersaturated solutions. The discharge of sodium ions from supersaturated solutions occurs when E is more negative than E_{sat} to E_{Na}. In the decomposition of supersaturated solutions, a 5-fold degree of supersaturation of the electrolyte in sodium is achieved. During the formation and decomposition of metallic sodium nuclei, it increases by more than 20 times and becomes sufficient to intensify and prolong the electrolysis process, to lower the lower limit of its realization temperature from 600 [17] to 350 °C.

The long-term region of potential constancy at $E_c = -2.97 \pm 0.01$ V is associated with the coexistence of saturated and supersaturated sodium solutions in the electrolyte in the near-cathode layer. The decomposition of the latter stabilizes the cathode potential. At $\lg Q = 2.41$, the entire supersaturated solution is consumed, the reactivity of sodium and the cathode potential drop sharply, and the discharge of sodium ions from diluted solutions starts at potentials from E_{sat} to values 0.25—0.35 V more positive.

It can be seen that the reducing ability of the melt decreases as the amount of electricity passed through, and hence as the amount of titanium powder accumulated in the electrolyte increases.

The formation of titanium metal in the near-anode space is explained by the disproportionation of Ti^{2+} ions entering the anode electrolyte from the near-anode layer and the near-cathode melt.

The resulting product is similar to powder [17], and after classification and spheroidization by gas atomization methods [18—24], it can be used for 3D printing as a starting material.

Refernces

1. *Niinomi M., Nakai M., Hieda J.* Development of new metallic alloys for biomedical applications. *Acta Biomater.* 2012. Vol. 11. P. 3888—3903. DOI: 10.1016/j.actbio.2012.06.037.
2. *Vaezi M., Yang S.* Extrusion-based additive manufacturing of PEEK for biomedical applications. *Virtual Phys. Prototyp.* 2015. Vol. 10. No. 3. P. 123—135. DOI: 10.1080/17452759.2015.1097053.
3. *Hiroyasu K., Yoshimasa T., Hideyuki I., Tatsushi K., Takayuki Y.* Application of titanium and titanium alloys to fixed dental prostheses. *J. Prosthodontic Res.* 2019. Vol. 565. P. 266—270. DOI: 10.1016/j.jpor.2019.04.011.
4. *Смирнов М.В.* Электродные потенциалы в расплавленных хлоридах. М.: Наука, 1973.
   Smirnov M.V. Electrode potentials in molten chlorides. Moscow: Nauka, 1973 (In Russ.).
5. *Smirnov M.V., Chebykin V.V., Tsiovkina L.A.* The thermodynamic properties of sodium and potassium dissolved in their molten chlorides, bromides, and iodides. *Electrochim Acta.* 1981. Vol. 26. No. 9. P. 1275—1288. DOI: 10.1016/0013-4686(81)85111-0.
6. *Ковалевский Р.А., Чебыкин В.В.* Транспортные характеристики восстановленных форм катионов растворителя в расплавах хлоридов щелочных металлов. *Расплавы.* 1992. No. 3. С. 36—42.
   Kovalevskii P.A., Chebykin V.V. Transport characteristics of reduced forms of solvent cations in melts of alkali metal chlorides. *Rasplavy.* 1992. No. 3. P. 36—42 (In Russ.).
7. *Fang Z.Z., Paramore J.D., Sun P., Ravi Chandran K.S., Zhang Y., Xia Y., Cao F., Koopman M., Free M.* Powder metallurgy of titanium — past, present, and future. *Int. Mater. Rev.* 2018. Vol. 63. No. 7. P. 407—459. DOI: 10.1080/09506608.2017.1366003.
8. *Dutta B., Froes F.H.* Additive manufacturing of titanium alloys. Butterworth-Heinemann, 2016. DOI: 10.1016/B978-0-12-804782-8.00002-1.
9. *Polyakov V.V., Babin A.V., Lebedev V.A.* Volumetric reduction of $FeCl_2$—$CaCl_2$ melt with calcium dissolved in calcium chloride. *Russ. J. Non-Ferr. Met.* 2019. Vol. 60. No. 4. P. 408—412. DOI: 10.3103/S1067821219040114.
10. *Лебедев В.А., Поляков В.В.* Способ получения микроструктурных порошков титана: Пат. RU2731950C2 (РФ). 2020.
    Lebedev V.A., Polyakov V.V. The method of obtaining microstructural titanium powders. Pat. RU2731950C2 (RF). 2020 (In Russ.).
11. *Лебедев В.А., Бабин А.В., Поляков В.В., Рымкевич Д.А., Бездоля И.Н.* Восстановление титана из его тетрахлорида кальцием, растворенным в расплаве $CaCl_2$. *Титан.* 2017. No. 1. С. 4—9.
    Lebedev V.A., Babin A.V., Polyakov V.V., Rymkevich D.A., Bezdolya I.N. Reduction of titanium from its tetrachloride calcium dissolved in the melt of the $CaCl_2$. *Titan.* 2017. No. 1. P. 4—9 (In Russ.).
12. *Лебедев В.А.* Взаимосвязь стандартных и условных стандартных потенциалов в расплавленных галогенидах. *Докл. Акад. наук СССР.* 1993. Т. 330. No. 5. С 586—589.
    Lebedev V.A. Relationship of standard and conventional standard potentials in molten halides. *Doklady Akademii nauk SSSR.* 1993. Vol. 330. No. 5. P. 586—589 (In Russ.).
13. *Храмов А.П., Чернышев А.А., Исаков А.В., Зайков Ю.П.* Вторичное восстановление тугоплавкого металла у гладкого катода при электролизе солевого расплава. 1. Вывод базовых уравнений для модели процесса. *Электрохимия.* 2020. Т. 56. No. 9. С. 771—781. DOI: 10.31857/S0424857020090054.
    Khramov A.P., Chernyshev A.A., Isakov A.V., Zaykov Yu.P. Secondary reduction of a refractory metal near a smooth cathode during electrolysis of molten salt. 1. Derivation of basic equations for the process model. *Russ. J. Electrochem.* 2020. Vol. 56. P. 699—708. DOI: 10.1134/S1023193520090050.
14. *Храмов А.П., Чернышев А.А., Исаков А.В., Зайков Ю.П.* Вторичное восстановление тугоплавкого металла у гладкого катода при электролизе солевого расплава. 2. Расчеты для некоторых гипотетических экспериментов. *Электрохимия.* 2020. Т. 56. No. 9. С. 782—787. DOI: 10.31857/S0424857020090066.
    Khramov A.P., Chernyshev A.A., Isakov A.V., Zaykov Yu.P. Secondary reduction of a refractory metal near a smooth cathode during electrolysis of molten salt. 2. Calculations for some hypothetical experiments. *Russ. J. Electrochem.* 2020. Vol. 56. P. 709—714. DOI: 10.1134/S1023193520090062.
15. *Вараксин А.В., Лисин В.Л., Костылев В.А.* Влияние параметров электрохимического процесса на гранулометрический состав и морфологию титановых порошков. *Бутлеровские сообщения.* 2014. Т. 37. No. 1. С. 62—67.
    Varaksin A.V., Lisin V.L., Kostylev V.A. The influence of the parameters of the electrochemical process on the particle size distribution composition and the morphology of titanium powders. *Butlerovskie soobshcheniya.* 2014. Vol. 37. No. 1. P. 62—67 (In Russ.).
16. *Барабошкин А.Н.* Электрокристаллизация металлов из расплавленных солей. М.: Наука, 1976.
    Baraboshkin A.N. Electrocrystallization of metals from molten salts. Moscow: Nauka, 1976 (In Russ.).

17. *Лебедев В.А., Поляков В.В.* Получение тонкодисперсного порошка титана объемным восстановлением его ионов натрием, растворенным в расплаве $BaCl_2$—$CaCl_2$—NaCl. *Известия вузов. Порошковая металлургия и функциональные покрытия*. 2022. No. 1. С. 4—16.
Lebedev V.A., Polyakov V.V. Production of finely dispersed titanium powder by volumetric reduction of its ions with sodium dissolved in the $BaCl_2$—$CaCl_2$—NaCl melt. *Izvestiya Vuzov. Poroshkovaya Metallurgiya i Funktsional'nye Pokrytiya (Powder Metallurgy and Functional Coatings)*. 2022. Vol. 16. No. 1. P. 4—16 (In Russ.).
18. *Boulos M.* Plasma power can make better powders. *Met. Powder Report*. 2004. Vol. 59. No. 5. P. 16—21. DOI: 10.1016/S0026-0657(04)00153-5.
19. *Sun P., Fang Z., Zhang Y., Xia Y.* Review of the methods for production of spherical Ti and Ti alloy powder. *J. Miner. Met. Mater. Soc.* 2017. Vol. 69. No. 10. P. 1853—1860. DOI: 10.1007/s11837-017-2513-5.
20. *Heidloff A.J., Rieken J.R., Anderson I.E., Byrd D., Sears J., Glynn M., Ward R.M.* Advanced gas atomization processing for Ti and Ti alloy powder manufacturing. *J. Miner. Met. Mater. Soc.* 2010. Vol. 62. No. 5. P. 35—41. DOI: 10.1007/s11837-010-0075-x.
21. *Larouche F., Balmayer M., Trudeau-lalonde F.* Plasma atomization metal powder manufacturing processes and systems therefore: Pat. WO2017011900 A1 (WIPO). 2017. https://patents.google.com/patent/WO2017011900A1/en?oq=WO2017011900+A1.
22. *Dion C.A.D., Kreklewetz W., Carabin P.* Plasma apparatus for the production of high quality spherical powders at high capacity: Pat. WO2016191854 A1 (WIPO). 2016. https://patents.google.com/patent/US20180169763A1/en?oq=WO2016191854+A1.
23. *Sun P., Fang Z., Xia Y., Zhang Y., Zhou C.* A novel method for production of spherical Ti—6Al—4V powder for additive manufacturing. *Powder Technol.* 2016. Vol. 301. P. 331—335. DOI: 10.1016/j.powtec.2016.06.022.
24. *Chen G., Zhao S., Tan P., Wang J., Xiang C., Tang H.* A comparative study of Ti—6Al—4V powders for additive manufacturing by gas atomization, plasma rotating electrode process and plasma atomization. *Powder Technol.* 2018. Vol. 333. P. 38—46. DOI: 10.1016/j.powtec.2018.04.013.